Applied Surface Science 388 (2016) 288–293

Contents lists available at ScienceDirect

Applied Surface Science

journal homepage: www.elsevier.com/locate/apsusc

Light-emitting structures of CdS nanocrystals in oxidized macroporous silicon

L. Karachevtseva[a,b,*], S. Kuchmii[c], O. Stroyuk[c], O. Lytvynenko[b], O. Sapelnikova[b], O. Stronska[b], Wang Bo[a], M. Kartel[a]

[a] Ningbo University of Technology, No. 55-155 Cui Bai Road, Ningbo 315016, China
[b] V. Lashkaryov Institute of Semiconductor Physics NAS of Ukraine, 41 Nauki pr., Kyiv 03028, Ukraine
[c] L. Pisarzhevsky Institute of Physical Chemistry NAS of Ukraine, 31 Nauki pr., Kyiv 03028, Ukraine

ARTICLE INFO

Article history:
Received 8 October 2015
Received in revised form 1 December 2015
Accepted 10 January 2016
Available online 12 January 2016

Keywords:
Photoluminescence
CdS nanocrystals
Oxidized macroporous silicon

ABSTRACT

Structured silicon substrates (macroporous silicon) with SiO_2 nanolayers and CdS nanocrystals were proposed to reduce the flow of electrons and recombination outside the nanoparticle layer. It was found that the resonance electron scattering in samples with low concentration of Si—O—Si states transforms into ordinary scattering on ionized impurities for samples with high concentration of Si—O—Si states. The maximal intensity of photoluminescence was measured for a structure with maximum strength of the local electric field at the Si—SiO_2 interface, indicating a significant decrease of non-radiative recombination in CdS nanocoating due to the flow of electrons from the silicon matrix towards the CdS nanocrystal layer. The quantum yield of photoluminescence increases with time due to evaporation of water molecules.

1. Introduction

Currently considerable interest exists in the light-emitting semiconductor nanocrystals based on II–VI compounds. This is due to the successes achieved by colloid chemistry in the synthesis of such structures [1]. The ability to control the optical properties by varying the nanocrystal size allows the development of "white" light sources, radiation converters and inorganic LEDs. The researches in this area are aimed at the development of nanocrystals in a dielectric matrix to reduce non-radiative recombination. The dependence of photoluminescence of CdSe nanoparticles and CdSe/ZnS on the matrix material (substrate) was studied on the basis of organic semiconductors and quartz [2].

Due to their size-tunable physical properties nanoscale semiconductor materials have promising applications, including the optoelectronic devices such as light-emitting diodes [3] and next generation quantum dot solar cells [4]. Moreover, nanoscale semiconductors functionalized with biomolecules are promising as molecular fluorescent probes in biological applications [5]. The deposition of light-emitting nanocrystals on structured silicon substrates will favor development of new waveguide amplifiers and lasers for silicon micro- and nanophotonics.

In this paper, oxidized macroporous silicon structures with CdS surface nanocrystals were proposed to reduce the flow of electrons and recombination outside the nanoparticles. In particular, the analysis of oxidized macroporous silicon structures with CdS nanoparticles was made on the basis of measurements of IR absorption spectra. Macroporous silicon is a promising material for the development of 2D photonic structures with the required geometry and large effective surface [6,7]. This determines the optical and electro-optical characteristics of macroporous silicon structures [8,9]. Thus the local electric field at the "macroporous silicon-nanocoating" interface was determined. And the influence of electric field on the photoluminescence intensity of CdS nanoparticles on oxidized silicon macroporous structures was evaluated.

2. Procedure

CdS nanocrystals were deposited onto silicon substrates from colloidal solution with polyethylenimine (PEI). The CdS nanocrystal size values were obtained from the data given by atomic force microscopy. A layer of 1.8/2 nm CdS nanoparticles (Fig. 1a) was deposited from a colloidal solution with PEI onto the oxidized macroporous silicon structure.

* Corresponding author at: V. Lashkarev Institute of Semiconductors Physics NAS of Ukraine, 41 Nauki pr., Nauki, 03028 Kyiv, Ukraine. Tel.: +380 44 525 23 09; fax: +380 44 525 83 42.
E-mail addresses: lakar@isp.kiev.ua (L. Karachevtseva), stephan@ukr.net (S. Kuchmii), alstroyuk@ukr.net (O. Stroyuk), lytvole@gmail.com (O. Lytvynenko), e_kolesnik84@mail.ru (O. Sapelnikova), yaschichek@ukr.net (O. Stronska), bo305@hotmail.com (W. Bo), nikar@kartel.kiev.ua (M. Kartel).

http://dx.doi.org/10.1016/j.apsusc.2016.01.069
0169-4332/

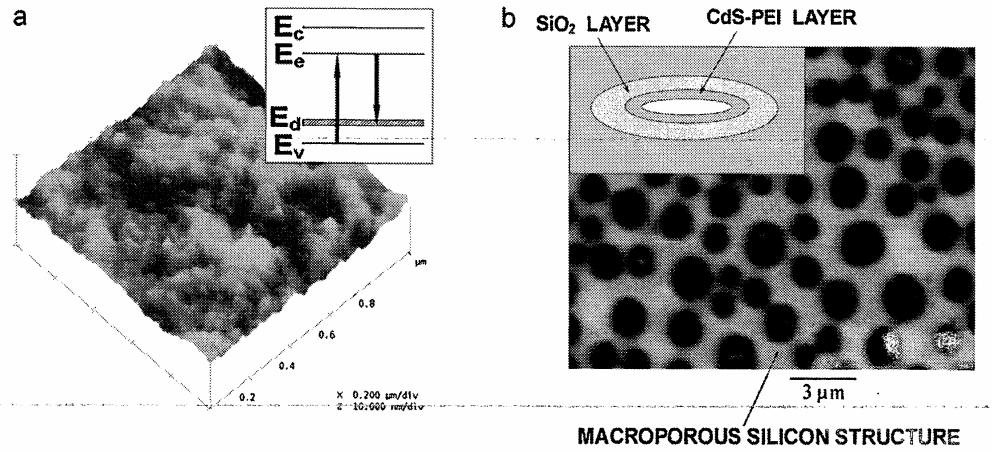

Fig. 1. (a) Morphology of CdS nanocrystals in PEI according to the data of atomic force microscopy. Inset: the photoluminescence band diagram with $E_c - E_v = 4.5$ eV (band-to-band excitation), $E_e - E_v = 3.44$ eV (exciton energy), $E_e - E_d \approx 2.7$ eV (defect level energy) [1,7]. (b) A fragment of the macroporous silicon structure with arbitrary distribution of macropores and direction of light incidence on the sample (along the main axis of cylindrical macropore).

Macroporous silicon structures with arbitrary distribution of macropores (Fig. 1b) were made of *n*-silicon wafers of [100] orientation (the electron concentration $n_0 = 10^{15}$ cm^{-3}) using photoelectrochemical etching [7]. The structures with macropore depth $h_p = 40$–80 μm, diameter $D_p = 2$–5 μm and concentration $N_p = (1$–$6) \times 10^6$ cm^{-2} were etched.

SiO_2 nanocoatings were formed in the diffusion stove after treatment in the nitrogen atmosphere. The oxide layers (thickness of 5–200 nm) were formed on macroporous silicon samples in dry oxygen for 40–60 min at a temperature of 1050 °C. The oxide thickness was measured using ellipsometry.

The chemical states on the surface of macroporous silicon structures with nanocoatings and the electric field at the "Si—SiO_2" boundary were identified by IR absorption spectra using a PerkinElmer Spectrum BXII IR Fourier spectrometer in the 300–8000 cm^{-1} spectral range. The optical absorption spectra were recorded at normal incidence of IR radiation on the sample (along the main axis of cylindrical macropores—see Fig. 1b). The experiments were carried out in air at room temperature.

The photoluminescence spectra of the macroporous silicon samples with a silicon oxide layer and CdS nanoparticles with PEI were obtained in the 1.8–3.3 eV range of photon energy. The excitation radiation with photon energy $E_e = 3.44$ eV of the first exciton peak [10] (see inset in Fig. 1a) falls on the sample through an optical fiber. And the photoluminescence emission of the test sample falls on the sensor and the optical fiber through a slit with width of 2.5 nm. The angle between the excitation radiation and photoluminescence emission is 5°.

3. Experimental

3.1. Macroporous silicon structures with SiO_2 nanocoatings

Preliminary surface cleaning of macroporous silicon with oxidation and oxide etching off reduces concentration of organic compounds, CH_2 and OH bonds. The IR absorption spectra of macroporous silicon structures after cleaning and further surface oxidation (oxide thickness of 5–200 nm) are shown in Fig. 2a. The IR absorption of macroporous silicon with surface oxide thickness of 5 nm (curve 2) is 1.5 times greater than that without surface oxidation (curve 1). The nature and intensity of absorption peaks are almost identical for curves 1 and 2.

The IR spectrum of the macroporous silicon sample with surface oxide thickness of 10 nm (curve 3) changes dramatically. We measured a 364 cm^{-1} peak of one-phonon absorption and 465 cm^{-1} peak associated with Si—O—Si rotation [11]. There is a strong growth of the Si—O—Si oxide peak (1095 cm^{-1}) with further oxidation of macroporous silicon (curves 4–7). This indicates increase of the concentration of bridge-like oxygen atoms in Si—O—Si (TO phonons) due to reduction of passivation of silicon and oxygen dangling bonds in the absence of hydrogen [12]. In addition to the TO phonon peaks (1086–1095 cm^{-1}), LO phonon absorption peaks (1250–1256 cm^{-1}) are formed due to radiation incidence along the surface of cylindrical macropores (geometry of frustrated total internal reflection [13]).

In addition, new absorption peaks are formed in the spectral regions of TO and LO phonons at $\omega = 1467$ cm$^{-1} = \omega_{LO} + (\omega_{LO} - \omega_{TO})$, 1646 cm$^{-1} = \omega_{LO} + 2(\omega_{LO} - \omega_{TO})$ and 1880 cm$^{-1} = \omega_{LO} + 3(\omega_{LO} - \omega_{TO})$, that are presented separately in Fig. 2b. A series of light absorption bands at $\omega \geq \omega_{LO}$ can be explained by formation of multi-phonon states [14] as a result of the interaction of phonons of the SiO_2 layer with waveguide modes in the silicon matrix. It is known that the surface LO phonons are phonon-polaritons [15], so the waveguide modes increase the density of the polariton multi-phonon states [16]. As a result, absorption increases as the frequency $(\omega_S^+)_N$ of the *N*th mode of surface phonon-polariton coincides with the frequencies of the waveguide modes. In our case, the guided and quasi-guided modes are formed on a silicon matrix with the parameters of modes equal to the spacing between the macropores [17,18]. According to Fig. 2, the resonance frequency *N*th mode of surface phonon polaritons is

$$\left(\omega_S^+\right)_N = \omega_{TO}\left[N\left(\frac{\varepsilon_0}{\varepsilon_\infty}\right)^{1/2} - (N-1)\right], \quad (1)$$

taking into account that the frequency of the LO phonon is $\omega_{LO} = \omega_{TO}(\varepsilon_0/\varepsilon_\infty)^{1/2}$ for p-polarized surface mode [14]. It should be noted that impurities increase the density of the polariton states too.

3.2. Comparison of the IR spectra of oxidized macroporous silicon with and without surface cleaning

Fig. 3a shows the IR spectra of macroporous silicon samples having surface oxide 200 nm thick, with (curve 1) and without (curves 2) surface cleaning.

Absorption of macroporous silicon samples without oxidation and oxide removal exceeds by 4–20 times that of macroporous silicon samples with previous cleaning. The oscillations of IR absorption (Fig. 3a and b) result from electron resonance scattering in a strong electric field by impurity states on the surface

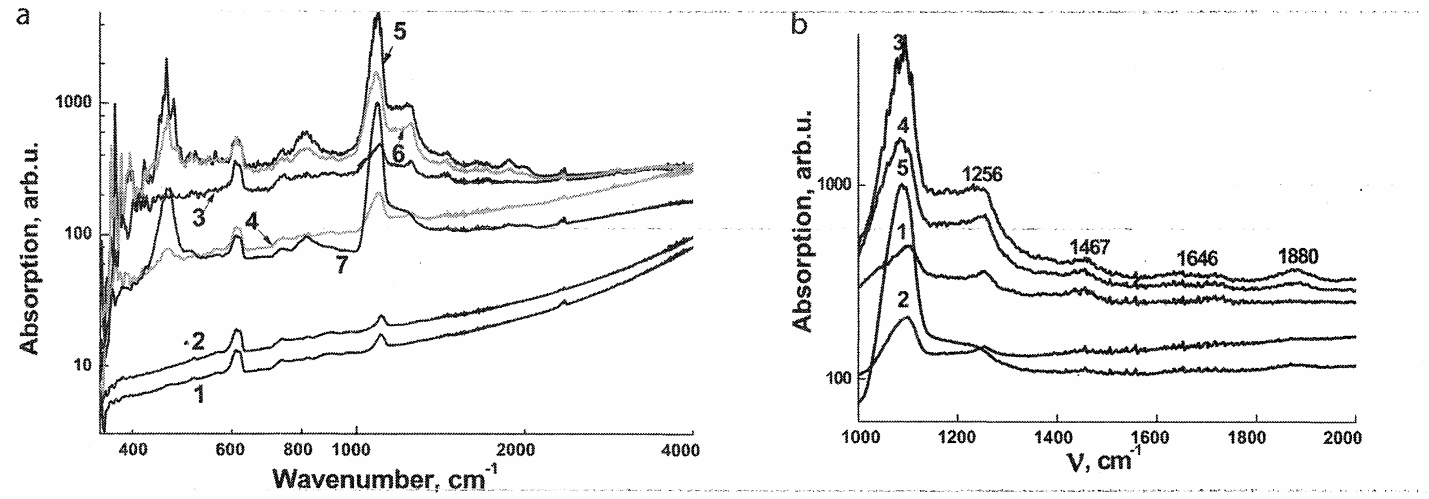

Fig. 2. (a) The IR spectra of macroporous silicon structures after surface cleaning without surface oxidation (curve 1) and with surface oxidation: oxide thickness of 5 nm (curve 2), 10 nm (curve 3), 20 nm (curve 4), 50 nm (curve 5), 100 nm (curve 6) and 200 nm (curve 7). (b) IR absorption spectra of macroporous silicon with surface oxide thickness of 10 nm (curve 1), 20 nm (curve 2), 50 nm (curve 3), 100 nm (curve 4) and 200 nm (curve 5) in the spectral region of TO and LO phonons.

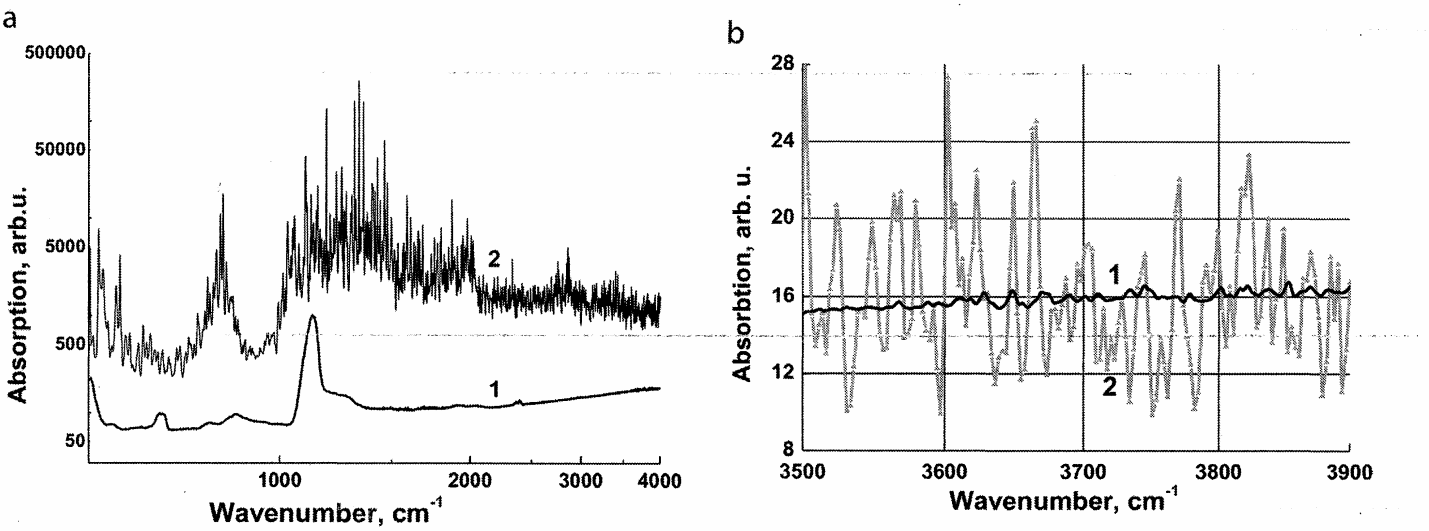

Fig. 3. (a) IR absorption spectra of macroporous silicon having surface oxide 200 nm thick, with (curve 1) and without (curve 2) surface cleaning. (b) Fragment of IR absorption spectra of macroporous silicon having surface oxide 200 nm thick, with (curve 1) and without (curve 2) surface cleaning.

of macropores, with the difference between two resonance energies $\Delta E = Fa = 8\text{–}20\ \text{cm}^{-1}$ equal to the Wannier–Stark step [18,19]. The oscillations (Fig. 3a) have small amplitudes of IR absorption and nearly the same period for samples with surface cleaning and those of macroporous silicon without previous surface cleaning (Fig. 3b).

Sharp decrease of the oscillation amplitude in the electro-optical effects is determined by an increase of the broadening parameter Γ [20]. The calculations of the broadened electro-optical function for the Franz–Keldysh effect were performed in [20,21]. By analogy with this approach, we determined the effect of broadening on the amplitude of oscillations in IR absorption spectra (ΔA) in the form of convolution of the "non-broadened" oscillation amplitude (ΔA_0) with the Lorentz distribution:

$$\frac{\Delta A}{\Delta A_0} = \frac{\Gamma}{\pi}\int \frac{d\omega'}{(\omega' - \omega)^2 + \Gamma^2} = \arctan\frac{(\Delta\omega/\Gamma)}{\pi}; \quad (2)$$

where $\Delta\omega = \omega' - \omega$ is the energy of the Wannier–Stark step Fa.

The results of calculation with Eq. (2) are shown in Fig. 4a, from which it follows that the oscillation amplitude increases linearly with Fa/Γ up to $Fa/\Gamma \approx 1$. The Fa/Γ values lie within $1 < Fa/\Gamma < 100$ for the experimental data on IR absorption in macroporous silicon structures with oxide thicknesses of 50 and 200 nm in the spectral region of the Si—O surface states (Fig. 2b) and $\Delta A/\Delta A_0 = 0.2\text{–}0.5$ (Fig. 3b). The same period of oscillations (see Fig. 2b) confirmed low values $\Gamma = 0.1\text{–}10\ \text{cm}^{-1}$. The obtained Γ values correspond to this parameter for surface phonon polaritons measured in thin films of II–VI semiconductors [18,22].

Let us analyze the dependencies of oscillation amplitudes ΔA on absorption A for local surface states of macroporous silicon structures (Fig. 4b). The dependence $\Delta A(A)$ for macroporous silicon samples without surface cleaning is linear. And the dependencies $\Delta A(A)$ obey the "3/2 law" for the samples after surface cleaning. The obtained dependencies of oscillation amplitudes ΔA on absorption A correspond to $\Gamma^{-1} \sim \tau \sim E$ or $E^{3/2}$ (where $\tau = \hbar/\Gamma$ is electron scattering lifetime and E is electron energy). The resonance scattering of oxidized macroporous silicon samples without preliminary surface cleaning with $\tau_r \sim E$ transforms into an ordinary electron scattering by ionized impurities with lifetime $\tau_I \sim E^{3/2}$ for the samples with surface cleaning.

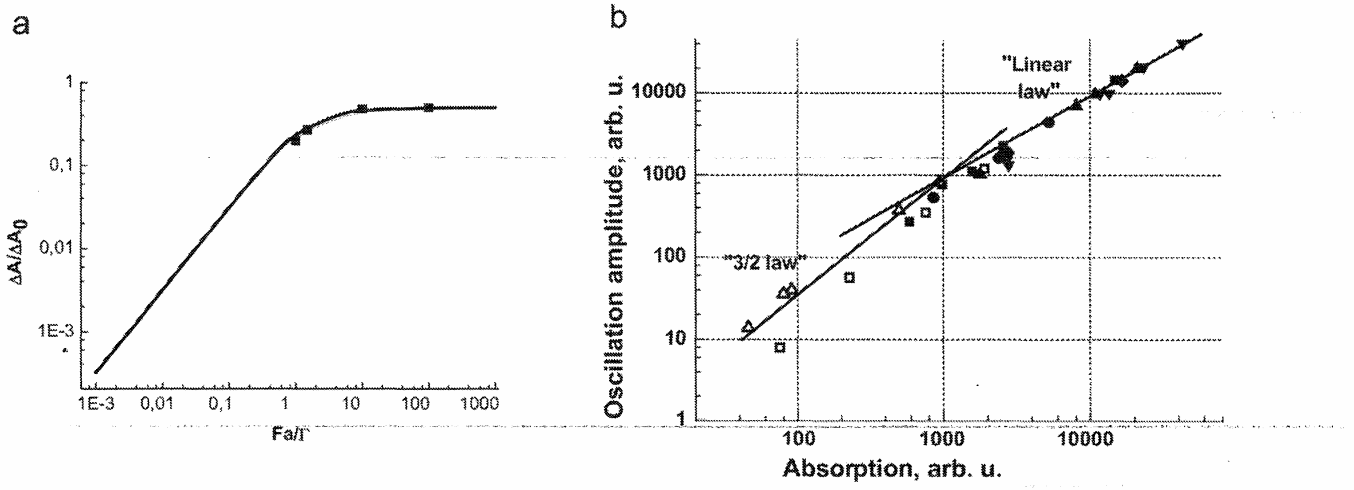

Fig. 4. (a) The results of calculation (curve) of the $\Delta A/\Delta A_0$ dependence on Fa/Γ by Eq. (2). The symbols are experimental data from Fig. 3a on IR absorption by macroporous silicon structures with oxide thicknesses of 50 and 200 nm in the spectral region of Si—O—Si surface states. (b) Dependencies of oscillation amplitudes on absorption for local surface states of macroporous silicon samples with SiO_2 nanocoatings after preliminary surface cleaning (open symbols) and without surface cleaning (fulled symbols).

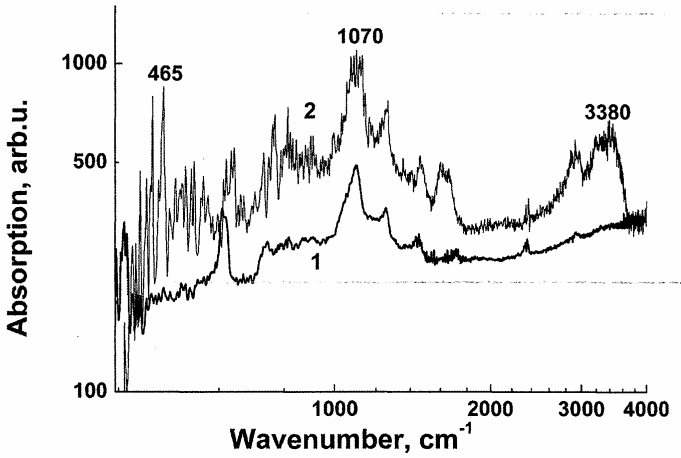

Fig. 5. The infrared absorption spectra of oxidized macroporous silicon structures without (1) and with (2) a nanolayer of CdS nanoparticles 30 nm thick and the oxide thickness 10 nm.

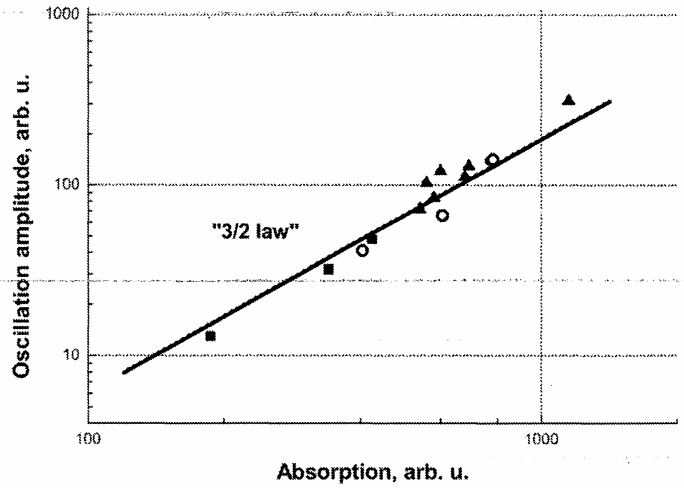

Fig. 6. Dependencies of oscillation amplitudes (ΔA) on absorption (A) for macroporous silicon samples with CdS nanocrystals and with the silicon oxide thicknesses 5 nm (■), 10 nm (○) and 20 nm (▲) for surface Si—O bonds.

Thus, the effect of broadening on the amplitude of oscillations in the IR absorption spectra is due to interaction of the surface multi-phonon polaritons with scattered electrons. This interaction transforms the resonance electron scattering (τ_r) in the samples without preliminary surface cleaning into scattering on ionized impurities (τ_I) for the samples with preliminary surface cleaning and the structured oxide formation.

3.3. Photoluminescence spectra

IR spectra and photoluminescence were investigated for oxidized macroporous silicon structures with preliminary surface cleaning and the layers of CdS nanocrystals with thickness of 10–30 nm and oxide thickness of 5–20 nm. Fig. 5 shows the IR absorption spectra of oxidized macroporous silicon structures without (curve 1) and with (curve 2) a nanolayer of CdS nanoparticles 30 nm thick and the oxide thickness 10 nm. IR absorption of oxidized macroporous silicon structures with a layer of CdS nanoparticles increases in comparison with that of oxidized macroporous silicon structures without a layer of CdS nanoparticles.

The obtained dependencies of oscillation amplitudes ΔA on absorption A (Fig. 6) correspond to scattering of electrons by ionized impurities with $\tau_I \sim E^{3/2}$. That scattering increases the flow of electrons from the silicon matrix towards the CdS nanocrystal layer in comparison with the resonance scattering with $\tau_r \sim E$. Thus, the deposition of a nanolayer of CdS increases IR absorption in comparison with IR absorption of oxidized macroporous silicon structures without a layer of CdS nanoparticles and saves mechanism of the electron scattering on ionized surface states.

The dependences of the spectral position of oscillation maxima (Fig. 5) in macroporous silicon with CdS nanoparticles are linear. The corresponding electric field strength ($F = \Delta E/a$) varies from 4.5×10^4 V/cm to 6.8×10^4 V/cm (Table 1).

Table 1
The electric field strength for oxidized macroporous silicon structures with CdS nanoparticles.

d_{CdS} (nm)	d_{SiO_2} (nm)	$F_S \times 10^{-4}$ (V/cm)
10	10	4.5
	20	4.9
20	10	5.8
	20	5.7
30	10	6.8
	20	6.4

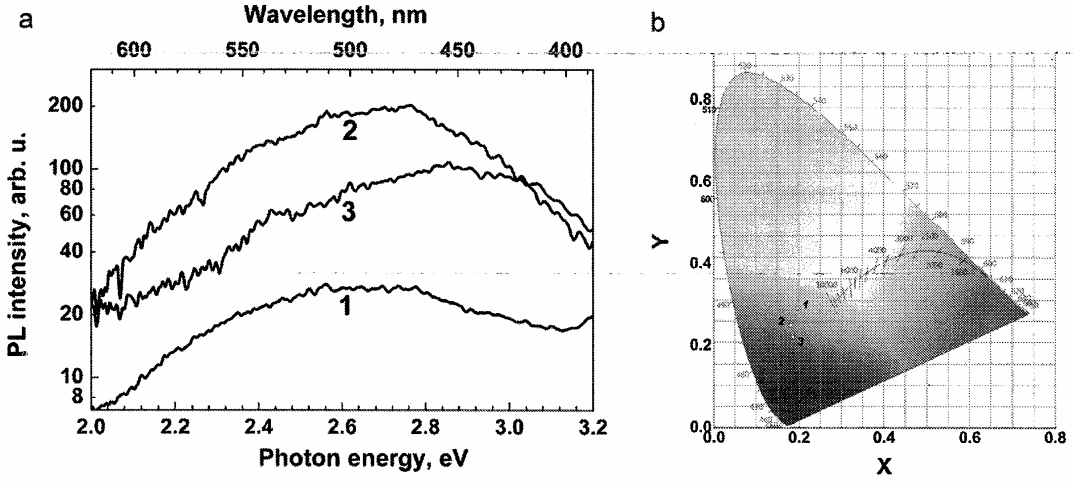

Fig. 7. (a) Spectral dependence of photoluminescence intensity in the macroporous silicon structures with CdS nanocrystal layer 30 nm thick and with the oxide layer thickness 5 (1), 10 (2) and 20 nm (3). (b) The CIE *x*–*y* chromaticity diagram with chromatical coordinates of the samples 1–3 from (a).

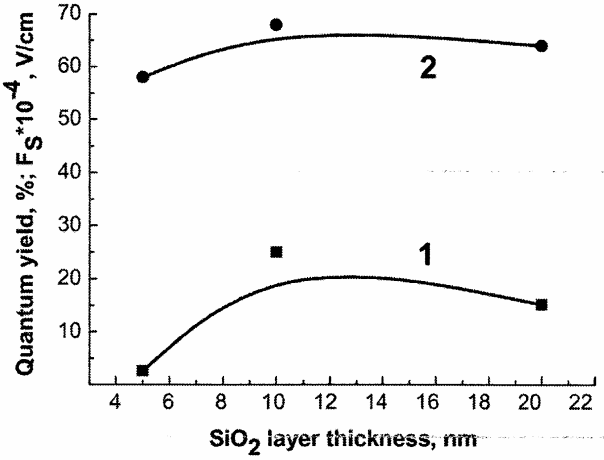

Fig. 8. The photoluminescence quantum yield (1) and electric field strength (2) vs. the SiO_2 thickness in macroporous silicon structures with CdS nanocrystal layer 30 nm thick.

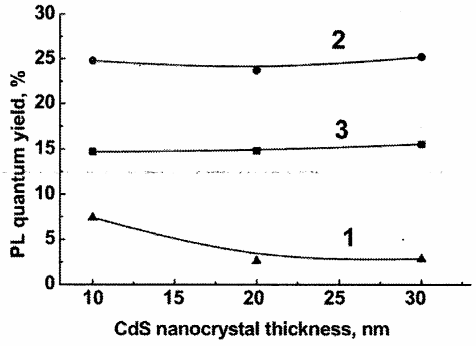

Fig. 9. The photoluminescence quantum yield vs the CdS nanocrystal thickness in macroporous silicon structures without silicon oxide (1), with oxide thickness of 10 nm (2) and 20 nm (3).

Fig. 7a shows the spectral dependence of photoluminescence intensity in macroporous silicon structures with CdS nanocrystals (thickness of 30 nm), the oxide thickness of 5, 10 and 20 nm. For structures of macroporous silicon with oxide thickness of 5 and 10 nm and CdS nanocrystals, the maximum of photoluminescence spectra (Fig. 7a, curves 1, 2) coincides with the corresponding data for aqueous colloidal solution of CdS-PEI (2.6–2.7 eV). For structures of macroporous silicon with oxide thickness of 20 nm and CdS nanocrystals, the maximum of photoluminescence spectra (Fig. 7a, curve 3) is shifted to higher energies. This indicates a decrease in the distance between the pairs of opposite charges localized in the "deep" traps [23].

Fig. 7b shows the CIE *x*–*y* diagram with chromaticity coordinates of the samples 1–3 from Fig. 7a. The color purity is 49.8% for sample 1, 59.1% (sample 2) and 60.4% (sample 3). The maximal color purity for sample 3 is due to the maximum photoluminescence spectra shift to higher energies.

The maximum intensity of the CdS nanoparticle photoluminescence was measured for structures with the highest strength of the local electric field at the Si–SiO_2 interface (Fig. 8). This indicates a significant decrease of non-radiative recombination of electrons generated on CdS nanocrystals due to the counter flow of electrons from the silicon matrix towards the CdS nanocrystal layer. The maximum of the photoluminescence intensity was measured for the structure of macroporous silicon with CdS nanocrystal layer 30 nm thick and oxide thickness of 10 nm. This structure has the highest electric field strength $F_S = 6.8 \times 10^5$ V/cm (Table 1) at the Si–SiO_2 interface.

Fig. 9 shows the dependence of the photoluminescence quantum yield on the CdS nanocrystal thickness for macroporous silicon structures without silicon oxide (1), with oxide thickness of 10 nm (2) and 20 nm (3). The photoluminescence quantum yield does not change for macroporous silicon structures with optimal oxide thickness of 10 and 20 nm and decreases for macroporous silicon structures without silicon oxide layer.

Photoluminescence spectra and photoluminescence quantum yield were measured over 7 and 14 days after the sample preparation. The photoluminescence spectral maximum increases by 4–6 times through 7 days after the sample preparation. That indicates a decrease in the rate of non-radiative recombination at the nanocoating as a result of decrease in the concentration of recombination centers in this area of structures. In addition, the spectral maximum shifts due to redistribution with time the density of nanoparticles in the CdS-PEI nanocoating.

The photoluminescence quantum yield of CdS nanoparticles on the surface of oxidized macroporous silicon with optimum thickness of SiO_2 layer increases by 1.5–2.3 times (Fig. 10) and reaches 28%. With further storage of samples, the photoluminescence quantum yield almost does not change. The quantum yield of photoluminescence for such structures increases with time due to evaporation of water molecules from the CdS-PEI layer [24].

The obtained value of the photoluminescence quantum yield for investigated nanostructures is comparable with those for CdS

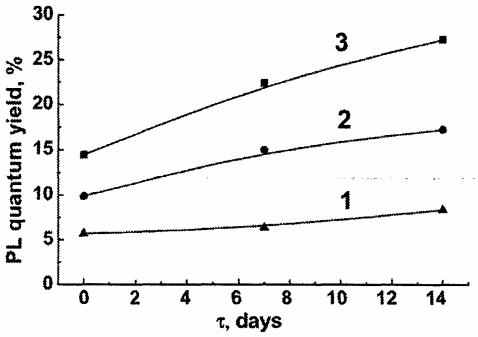

Fig. 10. Time dependence of the photoluminescence quantum yield in macroporous silicon structures with oxide thickness of 10 nm and CdS nanocoating 10 nm (1), 20 nm (2) and 30 nm (3) thick.

quantum dots (29%) after annealing process [25] and for 2–3 nm CdS quantum dots (26–27%) [5].

4. Conclusions

Macroporous silicon structures with SiO_2 nanolayers and CdS nanocrystals are proposed to enhance the photoluminescence of CdS nanoparticles due to reducing the electron recombination outside the nanoparticle layer.

It was found that the resonance electron scattering at the Si—SiO_2 interface for samples with low concentration of Si—O—Si states in oxide layer transforms into scattering on ionized surface states for samples with high concentration of Si—O—Si states in the structured oxide.

The deposition of a nanolayer of CdS onto oxidized macroporous silicon structures (i) increases IR absorption in comparison with that in structures without a layer of CdS nanoparticles and (ii) saves the mechanism of electron scattering on ionized surface states. This increases the flow of electrons from the silicon matrix towards the CdS nanocrystal layer.

The maximum intensity of the CdS nanoparticle photoluminescence was measured for structures with the highest strength of local electric field at the Si—SiO_2 interface. This indicates a significant decrease in non-radiative recombination of electrons generated on CdS nanocrystals due to the counter flow of electrons from the silicon matrix towards the CdS nanocrystal layer.

The photoluminescence quantum yield of CdS nanoparticles on the surface of oxidized macroporous silicon with optimum thickness of SiO_2 layer increases by 1.5–2.3 times during the first two weeks owing to evaporation of water molecules from nanoparticles in the polymer layer. With further storage of samples, the photoluminescence quantum yield almost does not change.

Acknowledgments

This work was supported by the State Program of National Academy of Sciences of Ukraine 'Nanotechnologies and Nanomaterials', Project # 6.22.2.15.

References

[1] A.E. Raevskaya, A.I. Stroyuk, S. Ya. Kuchmii, Optical characteristics of colloidal nanoparticles CdS stabilized with sodium polyphosphate and their behavior during pulse photoexcitation, Theor. Exp. Chem. 39 (2003) 158–165.
[2] A.A. Chistyakov, et al., Interaction of CdSe/ZnS core–shell semiconductor nanocrystals in solid thin films, Laser Phys. 16 (2006) 1625–1632.
[3] T. Trindade, P. O'Brien, N.L. Pickett, Nanocrystalline semiconductors: synthesis, properties, and perspectives, Chem. Mater. 13 (2001) 3843–3858.
[4] Y. Shen, Y. Lee, Assembly of CdS quantum dots onto mesoscopic TiO_2 films for quantum dot-sensitized solar cell applications, Nanotechnology 19 (2008) 045602.
[5] J.J. Beato-López, C. Fernández-Ponce, E. Blanco, et al., Preparation and characterization of fluorescent CdS quantum dots used for the direct detection of GST fusion proteins, Nanomater. Nanotechnol. 2 (2012) 10, http://dx.doi.org/10.5772/53926.
[6] A. Birner, R.B. Wehrspohn, U.M. Gösele, K. Busch, Silicon-based photonic crystals, Adv. Mater. 13 (2001) 377–388.
[7] L.A. Karachevtseva, Two-dimensional photonic crystals as perspective materials of modern nanoelectronics, Semicond. Phys. Quantum Electron. Optoelectron. 7 (2005) 430–435.
[8] A. Glushko, L. Karachevtseva, Photonic band structure in oxidized macroporous silicon, Opto-Electron. Rev. 14 (2006) 201–203.
[9] L. Karachevtseva, V. Onyshchenko, A. Sachenko, Photocarrier transport in 2D macroporous silicon structures, Opto-Electron. Rev. 18 (2010) 394–399.
[10] W.W. Yu, L. Qu, W. Guo, X. Peng, Experimental determination of the extinction coefficient of CdTe, CdSe, and CdS nanocrystals, Chem. Mater. 15 (2003) 2854–2860.
[11] A.G. Cullis, L.T. Canham, P.D.J. Calcott, The structural and luminescence properties of porous silicon, J. Appl. Phys. 82 (1997) 909–965.
[12] N.H. Nickel, P. Mei, J.B. Boyce, On the nature of the defect passivation in polycrystalline silicon by hydrogen and oxygen plasma treatments, IEEE Trans. Electron Devices 42 (1995) 1559–1560.
[13] N.J. Harrick, Internal Reflection Spectroscopy, Interscience Publishers, New York/London/Sydney, 1967.
[14] E.A. Vinogradov, Semiconductor microcavity polaritons, Physics-Uspekhi 45 (2002) 1213–1250.
[15] F. Priox, M. Balkanski, Infrared measurements on CdS thin films deposited on aluminium, Phys. Status Solidi B: Basic Solid State Phys. 32 (1969) 119–126.
[16] E.A. Vinogradov, G.N. Zhizhin, V.A. Yakovlev, Resonance between dipole oscillations of atoms and interference modes in crystalline films, Sov. Phys. JETP 50 (1979) 486–490.
[17] L.A. Karachevtseva, V.I. Ivanov, O.O. Lytvynenko, K.A. Parshin, O.J. Stronska, The impurity Franz–Keldysh effect in 2D photonic macroporous silicon structures, Appl. Surf. Sci. 255 (2008) 3328–3331.
[18] L.A. Karachevtseva, S.Ya. Kuchmii, K.P. Konin, O.O. Lytvynenko, A.L. Stroyuk, Room temperature Wannier–Stark effect in 2D macroporous silicon structures with nanocoatings, Chemistry, Phys. Technol. Surf. 2 (2011) 105–113.
[19] L. Karachevtseva, S. Kuchmii, O. Lytvynenko, F. Sizov, O. Stronska, A. Stroyuk, Oscillations of light absorption in 2D macroporous silicon structures with surface nanocoatings, Appl. Surf. Sci. 257 (2011) 3331–3335.
[20] B.O. Seraphin, N. Bottka, Band-structure analysis from electro-reflectance studies, Phys. Rev. 145 (1966) 628–636.
[21] R. Enderlein, The influence of collisions on Franz–Keldysh effect, Phys. Stat. Sol. 20 (1967) 295–299.
[22] L.K. Vodopyanov, E.A. Vinogradov, V.V. Kolotkov, Yu.A. Mityagin, Optical properties of cadmium telluride in the far-IR, Sov. Phys. Solid State 16 (1974) 1419–1425 [in Russian].
[23] N. Chestnoy, T.D. Harris, R. Hull, L.E. Brus, Luminescence and photophysics of cadmium sulfide semiconductor clusters: the nature of the emitting electronic state, J. Phys. Chem. 90 (1986) 3393–3399.
[24] V.D. Pokhodenko, S.Ya. Kuchmii, A.V. Korzhak, A.I. Kryukov, Photochemical behavior of nanoparticles of cadmium sulfide in the presence of a reducing agent, Theor. Exp. Chem. 32 (1996) 88–92.
[25] J.I. Kim, J. Kim, J. Lee, et al., Photoluminescence enhancement in CdS quantum dots by thermal annealing, Nanoscale Res. Lett. 7 (2012) 482, http://dx.doi.org/10.1186/1556-276X-7-482.